zation to produce chain-folded single crystals and, as illustrated in the present study, epitaxial crystallization to orient a projection normal to the chain axis. Electron diffraction is required in this latter case due to the small size of chain-folded single crystals and also because the thickness of epitaxial layers (*ca* 30 nm) must be limited to avoid disorientation mechanisms linked with bulk polymer growth (*e.g.* lamellar twisting).

Research described in this paper was funded in part by a grant from the National Science Foundation (CHE 91-13899), which is gratefully acknowledged. (This grant is sponsored by both the Theoretical and Computational Chemistry and Polymers Programs of the NSF.)

References

BRISSE, F. (1989). *J. Electron Microsc. Techn.* **11**, 272–279.
BRISSE, F., RÉMILLARD, B. & CHANZY, H. (1984). *Macromolecules*, **17**, 1980–1987.
CHANZY, H., PÉREZ, S., MILLER, D. P., PARADOSSI, G. & WINTER, W. T. (1987). *Macromolecules*, **20**, 2407–2413.
COJAZZI, G., MALTA, V., CELOTTI, G. & ZANNETTI, R. (1976). *Makromol. Chem.* **177**, 915–926.
COWLEY, J. M. (1981). *Diffraction Physics*, 2nd ed. Amsterdam: North-Holland.
COWLEY, J. M. & KUWABARA, S. (1962). *Acta Cryst.* **15**, 260–270.
COWLEY, J. M. & MOODIE, A. F. (1959). *Acta Cryst.* **12**, 360–367.
COWLEY, J. M., REES, A. L. G. & SPINK, J. A. (1951). *Proc. Phys. Soc. London*, A**64**, 609–619.
DETITTA, G. T., EDMONDS, J. W., LANGS, D. A. & HAUPTMAN, H. (1975). *Acta Cryst.* A**31**, 472–479.
DORSET, D. L. (1976). *Acta Cryst.* A**32**, 207–215.
DORSET, D. L. (1980). *Acta Cryst.* A**36**, 592–600.
DORSET, D. L. (1991*a*). *Ultramicroscopy*, **38**, 23–40.
DORSET, D. L. (1991*b*). *Macromolecules*, **24**, 1175–1178.
DORSET, D. L. (1991*c*). *Proc. Natl Acad. Sci. USA*, **88**, 5499–5502.
DORSET, D. L. (1992*a*). *Macromolecules*, **25**, 4425–4430.
DORSET, D. L. (1992*b*). *Ultramicroscopy*, **45**, 357–364.
DORSET, D. L., MASSALSKI, A. M. & FRYER, J. R. (1987). *Z. Naturforsch. Teil A*, **42**, 381–391.
DORSET, D. L., TIVOL, W. F. & TURNER, J. N. (1992). *Acta Cryst.* A**48**, 562–568.
DOYLE, P. A. & TURNER, P. S. (1968). *Acta Cryst.* A**24**, 390–397.
GUIZARD, C., CHANZY, H. & SARKO, A. (1985). *J. Mol. Biol.* **183**, 397–408.
HAUPTMAN, H. & GREEN, E. A. (1976). *Acta Cryst.* A**32**, 45–49.
HU, H. & DORSET, D. L. (1989). *Acta Cryst.* B**45**, 283–290.
KARLE, I. L., DRAGONETTE, K. S. & BRENNER, S. A. (1965). *Acta Cryst.* **19**, 713–716.
KARLE, J. & HAUPTMAN, H. (1956). *Acta Cryst.* **9**, 635–651.
KOPP, S., WITTMANN, J.-C. & LOTZ, B. (1993). *Polymer*. In the press.
LANGS, D. A. & DETITTA, G. T. (1975). *Acta Cryst.* A**31**, 516.
MEILLE, S. V., BRÜCKER, S. & LANDO, J. (1989). *Polymer*, **30**, 786–792.
MOODIE, A. F. (1965). *Int. Conf. Electron Diffr. Cryst. Defects*, Melbourne, Australia, Paper ID-1.
PÉREZ, S. & CHANZY, H. (1989). *J. Electron Microsc. Techn.* **11**, 280–285.
SAYRE, D. (1952). *Acta Cryst.* **5**, 60–65.
VAINSHTEIN, B. K. (1956). *Sov. Phys. Crystallogr.* **1**, 117–122.
WILSON, A. J. C. (1942). *Nature (London)*, **150**, 151–152.
WITTMANN, J. C., HODGE, A. M. & LOTZ, B. (1983). *J. Polym. Sci. Polym. Phys. Ed.* **21**, 2495–2509.
WITTMANN, J. C. & LOTZ, B. (1990). *Prog Polym. Sci.* **15**, 909–948.

Acta Cryst. (1994). B**50**, 208–216

X-ray Diffraction Studies of Oriented Dilauroyl Phosphatidylcholine Bilayers in the L_δ and L_α Phases

BY J. KATSARAS,* R. H. STINSON AND J. H. DAVIS

Department of Physics, University of Guelph, Guelph, Ontario, Canada N1G 2W1

(*Received* 17 *April* 1993; *accepted* 4 *August* 1993)

Abstract

X-ray diffraction studies on oriented multilayers of dilauroyl phosphatidylcholine in the lyotropic liquid-crystalline L_α phase and a not previously reported mono-domain three-dimensional L_δ phase at two temperatures (293 and 343 K) and various relative humidities (0–100%) are described. Absolute one-dimensional electron-density profiles of the different structural phase bilayers were constructed to a resolution of 4 Å using direct methods (*e.g.* swelling and triplet structure-invariant relationships) to solve for the phase problem. The absolute electron-density distributions clearly demonstrate differences between the two structural phases of dilauroyl phosphatidylcholine bilayers. In addition, the various structural properties of the two different phases have been quantified. In the case of the L_δ phase, the structural quantities (*e.g.* volumes of the terminal methyl group and headgroup, and the number of waters) are examined for the first time.

* Present address for correspondence author: Centre de Recherche Paul Pascal-CNRS, Avenue A. Schweitzer, 33600 Pessac, France.

Introduction

Lipids have the remarkable capability of forming a variety of structures with periodicities in one, two or three dimensions (long-range organization), while at the same time exhibiting short-range disorder (Luzzati, Gulik-Krzywicki & Tardieu, 1968). Another prominent characteristic is their ability to undergo reversible thermotropic and lyotropic transitions. Since the interactions between hydrocarbon chains are of prime importance in the formation of many lipid phases, including the various lamellar phases, much effort has been put into characterizing the structure and polymorphism of the hydrocarbon chains in lipids (Small, 1984; Abrahamsson, Dahlen, Löfgren & Pascher, 1978; Tardieu, Luzzati & Reman, 1973). However, various structures (*e.g.* lamellar, hexagonal *etc.*) are also dependent on the type and size of the polar headgroups which become increasingly important with decreasing hydrocarbon-chain lengths (Abrahamsson *et al.*, 1978).

1,2-Diacylphosphatidylcholines (PC's) are lipids commonly found in animal cell membranes (Gennis, 1989). Some of these lipids, such as dipalmitoyl PC (DPPC, 16:0) and dimyristoyl PC (DMPC, 14:0), have been extensively studied using a variety of techniques (*e.g.* Katsaras & Stinson, 1990; Morrow & Davis, 1987; Chapman, Urbina & Keough, 1974). On the other hand, dilauroyl PC (DLPC, 12:0) has been the subject of very little scientific investigation. The hydrocarbon chains of DLPC are short and close to the minimum length required for the formation of a bilayer structure (Morrow & Davis, 1987), while the choline headgroup is rather bulky, making it an interesting phospholipid for a structural study.

X-ray diffraction has been applied to the study of many model membrane systems (*e.g.* Katsaras, Stinson, Davis & Kendall, 1991; Katsaras & Stinson, 1990; Tardieu *et al.*, 1973); to our knowledge, some of the most complete diffraction work on DLPC bilayers (and other model systems) was performed by Tardieu *et al.* (1973). They studied DLPC multilayers under various temperature and hydration combinations and observed that they can exist in a variety of one- and two-dimensional phases. One structural phase which was observed at high temperature and low water concentration was the lamellar L_δ phase for which electron-density profiles were constructed on a relative scale. This phase (L_δ) is characterized by a bilayered structure, the hydrocarbon chains of which are apparently helical (3.4 CH_2 groups per turn) and the phosphatidylcholine headgroups of which form a two-dimensional square lattice having an edge of 6.8 Å. DLPC along with egg-PC in 6% cetyltrimethyl ammonium bromide were the only two lipids which contained a pure L_δ phase. Doucet, Levelut & Lambert (1983) studied single crystals of DPPC under various temperature and pressure regimes in which they observed a three-dimensional L_δ (3D-L_δ) domain having a repeat spacing of 54 Å when the crystals of the lipid were placed in a vacuum and heated to 323 K. However, the diffraction patterns also contained reflections from a structure having a repeat spacing of 47 Å which Doucet *et al.* (1983) attributed to a two-dimensional L_δ phase.

The goal of an X-ray diffraction experiment is the construction of an electron-density map. From an X-ray diffraction pattern the amplitudes of the structure factors can be determined directly. However, the construction of the map also requires that the phases of the structure factors be known. The fact that the phases are not directly measurable constitutes the phase problem. In the present study, at 293 K the phase problem was solved by swelling the bilayers and calculating the continuous Fourier transforms at each swelling using Shannon's sampling theorem (Sayre, 1952; Shannon, 1949). At 343 K, the bilayers did not swell and the phase problem was solved using triplet structure-invariant relationships after defining the origin (center of symmetry) by fixing the phase of one reflection (Dorset, 1990).

In this paper we report studies which show that oriented DLPC bilayers will form a mono-domain 3D-L_δ phase at 343 K and 0% relative humidity (RH), the result of a stacking of two-dimensional ordered layers with correlation between successive layers (Doucet *et al.*, 1983). The bilayers also form a liquid-crystalline (L_α) phase at 343 K and RH's $\geq$ 30%, and at 293 K with RH's $\geq$ 55%. The absolute electron-density profiles, constructed to a resolution of 4 Å using various direct methods to obtain the phase portion of the structure factor, clearly demonstrate the structural differences between 3D-L_δ and L_α phase bilayers. In addition, we have quantified the various structural properties of the two different phases. In the case of the L_δ phase, the structural quantities (*e.g.* volumes of the terminal methyl group and headgroup, and the number of waters) are examined for the first time. Finally, the data clearly show the phosphorylcholine headgroup reorienting upon going from the L_δ to the L_α phase and in contrast to Tardieu *et al.* (1973), the hydrocarbon chains in 3D-L_δ phase bilayers are not helical.

Experimental

L-α-Dilauroyl phosphatidylcholine (DLPC) was obtained from Avanti Polar Lipids, Inc. (Birmingham, AL, USA) and used as supplied. Lipid purity was checked using thin-layer chromatography (TLC, developing solvent: $CHCl_3/CH_3OH/H_2O/NH_4OH$, 58:35:5.4:1.6) and observing a single non-diffuse spot.

DLPC bilayers were oriented by placing either lipid powder or a concentrated solution of DLPC/

methanol (24 h in a vacuum at room temperature to remove the methanol) on the surface of a glass tube which was placed in a 100% RH environment at 343 K. The sample was then annealed by cycling between 0 and 100% RH environments at 343 K with the 3D-L_δ phase being formed at 0% RH when the sample formed a clear film. TLC showed that this procedure did not cause a breakdown in the lipid. Oriented bilayers which were studied at 293 K were prepared in a similar fashion except they were annealed at room temperature.

The X-ray source and camera for the one-dimensional diffraction patterns have been previously described (Katsaras *et al.*, 1991; Katsaras & Stinson, 1990). Two-dimensional diffraction patterns were obtained with an *R*-axis IIC image-plate detector (Rigaku Corporation, Japan) having a pixel size of 105 × 105 μm and an effective detection area of 200 × 200 mm using a point source of Cu $K\alpha$ radiation from a Rigaku Rotaflex RU-200B series rotating-anode X-ray generator (Rigaku Corporation, Japan) operating at 4 kW (50 kV and 80 mA). Monochromation of the Cu radiation was achieved using a graphite crystal.

One-dimensional diffraction patterns were collected for 100 and 1000 s with intensities of the various diffraction peaks determined after background subtraction. Two-dimensional diffraction patterns were collected for 10 min. Measured intensities in general are corrected by multiplying by the square of the order number (h^2) for a powder pattern and by the order number (h) for oriented samples. These two intensity corrections are referred to as full-Lorentz and half-Lorentz corrections, respectively. Since our samples revealed a high degree of orientation, as indicated by the absence of any wide-angle contributions in the one-dimensional patterns and well defined reflections confined to the meridional axis in the two-dimensional diffraction patterns ($< 10°$ mosaicity), the intensities were scaled up by a factor of h alone. Additional intensity corrections for absorption and atomic scattering factors can also be made. In the present experiments sample thicknesses were estimated to be between 2.5 and 5 μm. Calculations show that at this range of thicknesses and with the radius of curvature of the glass sample tube used (outer diameter ≃ 18 mm), the two additional correction factors cancel each other and therefore need not be applied. For example, the decrease in intensity at higher orders as a result of the decrease in atomic scattering factors is compensated for by the increased transmission of these same reflections because of their shorter path length within the sample.

At 293 K, the DLPC bilayers were able to swell with increasing levels of hydration. The reflections were phased using the Shannon sampling theorem (Sayre, 1952; Shannon, 1949). However, there are two situations which exclude the swelling method from being used successfully: (*a*) The lipid multilayers cannot swell and as such the continuous transform cannot be mapped out; (*b*) the motif (lipid bilayer) is not preserved. The continuous transform can still be sampled at different reciprocal lattice points if the motif only undergoes small gradual changes (*e.g.* increasing tilt with increasing hydration; Katsaras, Yang & Epand, 1992; Torbet & Wilkins, 1976). At 343 K, the bilayers could not be induced to swell and in addition experienced a phase transition at about 30% RH. Consequently, the phase problem for these samples (343 K) was solved using triplet structure-invariant relationships (Dorset, 1990; Hauptman & Karle, 1953).

The technique employed in determining the phases for samples at 343 K and various RH's was based on a probability method whereby a set of equations for a centrosymmetric structure are created. In this set of equations, the magnitudes of the structure factors for the membrane and the atomic structure factors are assumed to be known. What are regarded as unknown are the phases for the membrane structure factors. The application of these Hauptman–Karle three-phase structure-invariant relationships relating to bilayers is explained in further detail in works by Dorset (1990) and Dorset, Beckmann & Zemlin (1990).

Electron-density distributions were translated to an absolute scale by knowing the absolute electron densities of any two points or regions in the profile (*e.g.* water layer, hydrocarbon region or the mean electron density) on the following basis: At 343 K and 0% RH (3D-L_δ phase), the diffraction pattern contains a 1/4.4 $Å^{-1}$ reflection indicative of an orthorhombic hydrocarbon-chain packing arrangement corresponding to an area of 19.0 $Å^2$ per hydrocarbon chain (Small, 1984; Ruocco & Shipley, 1982). Since the distance between alternate C atoms in a fully extended fatty-acid chain is 2.53 Å (Tanford, 1973), then the 20 CH_2 groups in DLPC have a total volume of ~481 $Å^3$. For the terminal methyl groups in the hydrocarbon tails we used a mean volume of 46 $Å^3/CH_3$ group (V_{CH_3}), while for the headgroup, including the glycerol backbone and the carbonyl groups, a volume of 348 $Å^3$ was employed (Nagle & Wiener, 1988). For the 343 K and 0% RH DLPC bilayers we also assigned 2.6 molecules of water per lipid molecule (Jendrasiak & Hasty, 1974), thus adding another 79.6 $Å^3$ to the total volume. From the above information, we calculated an approximate average bilayer electron density of 0.367 e $Å^{-3}$ from a DLPC lipid molecule of volume ~1001 $Å^3$ containing 368 e. In addition, the mean electron-density distribution along the fatty-acid tails (ρ_{CH_2}) was calculated to be ~0.33 e $Å^{-3}$, giving us the second measurement necessary to place the distributions on

an absolute scale. In the L_α phase, the electron-density profiles were placed on an absolute scale in a fashion similar to the 3D-L_δ phase with the following differences: (*a*) the volume of $CH_2 \simeq 27.6$ Å^3 (Nagle & Wiener, 1988); (*b*) the volume of $CH_3 \simeq 55.2$ Å^3 (Nagle & Wiener, 1988). From the above we obtain a mean bilayer density of ~ 0.34 e Å^{-3} with the hydrocarbon region having an average electron density of 0.29 e Å^{-3}. The number of waters per lipid was not taken into account in calculating the average electron density of the bilayers in the L_α phase since water at 293 K has an electron density of 0.334 e Å^{-3}.

Results and discussion

In Fig. 1 we present two-dimensional X-ray diffraction patterns of lamellar phase DLPC bilayers at 343 K and relative humidities of 0 (Figs. 1*a* and 1*c*) and 100% (Fig. 1*b*). The diffraction pattern in Figs. 1(*a*) and 1(*c*) are the result of 3D-L_δ phase DLPC bilayers having a repeat spacing (*d* spacing) of 44.2 Å. In addition to the meridional reflections (**c***), there exist Bragg reflections parallel to **c*** at inverse lattice spacings of 1/6.8 and 1/4.8 Å^{-1} [1:(2)$^{1/2}$:(4)$^{1/2}$ *etc.*] as a result of the phosphorylcholine headgroups forming a two-dimensional square lattice of edge ~ 6.8 Å with a coupling between successive bilayers. In a pure 2D-L_δ phase, the Bragg spots parallel to **c*** would appear only as diffuse lines. In contrast to the 2D-L_δ phase observed by Tardieu *et al.* (1973), there does not seem to be any evidence supporting the helical conformation of hydrocarbon chains when the DLPC bilayers are in the 3D-L_δ phase. To our knowledge, this phase has not been observed previously in DLPC and our electron-density maps of the L_δ phase differ significantly from that presented by Tardieu *et al.* (1973) which also contained a *d* spacing of 41.1 Å. Additionally, in the 3D-L_δ phase the hydrocarbon chains are in an orthorhombic packing, as indicated by an equatorially centered reflection at a distance of 1/4.4 Å^{-1} (Small, 1984; Ruocco & Shipley, 1982). At 100% RH (Fig. 1*b*), the wide-angle reflections (1/4.4 Å^{-1}) together with the reflections as a result of the packing of the hydrophilic headgroups in a square lattice disappear while the *d* spacing experiences a decrease of 2.8 Å giving 41.4 Å, indicative of lipid bilayers that have undergone a phase transition to the L_α phase.

From 30 to 100% RH, the *d* spacing of the DLPC multilayers remained relatively constant (± 0.1 Å), thus rendering the swelling method of phase determination inadequate. The swelling method assumes that the bilayers are capable of being swollen while the motif (bilayer) is preserved. In the 343 K temperature regime these conditions were not met and as such, the probability methods as described by Hauptman & Karle (1953) and later used by Dorset (1990; 1991*a*,*b*) on various bilayer systems were employed.

There are several direct-determination methods that one can apply to solve the phase problem (*e.g.* inequalities, equalities and probabilities) (Sherwood,

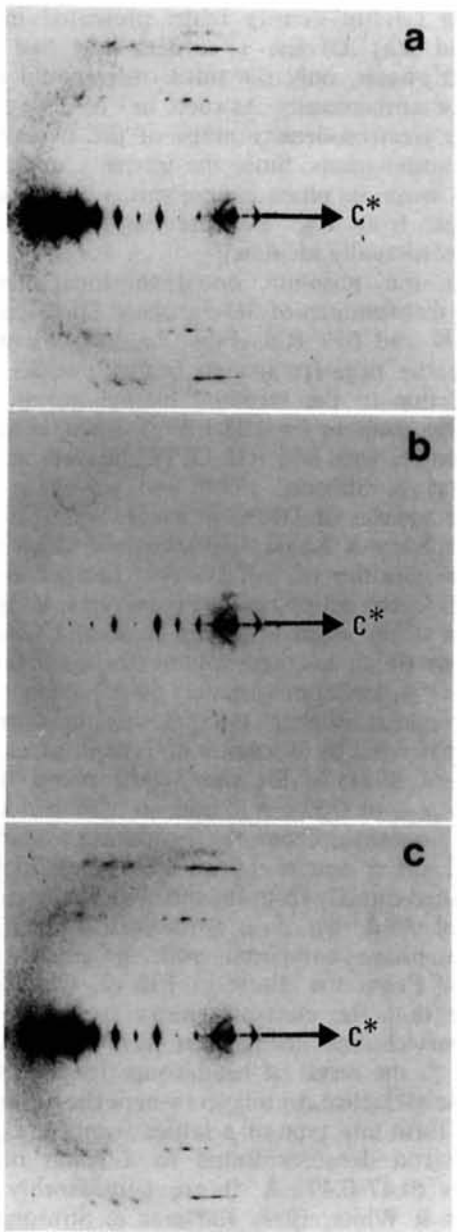

Fig. 1. Two-dimensional X-ray diffraction patterns of oriented DLPC bilayers at 343 K and: (*a*) 0% RH; (*b*) 100% RH; (*c*) 0% RH. The phase transitions from a 3D-L_δ phase at 343 K and 0% RH (*a*) to an L_α phase at 343 K and RH's $\geq$ 30%, (*b*) back to a 3*D*-L_δ phase and (*c*) occurs in the order of hours. The diffuse band extending from the **c*** axis in the wide-angle region is from the windows of the sample holder. The sample was placed on the outside of a 30 ml Pyrex beaker having an outer diameter of 35 mm.

1976). However, in this case the probability method was chosen because of its effectiveness with systems similar to those presented here (Dorset, 1990; 1991*a*,*b*). One-dimensional X-ray diffraction patterns from 3D-L_δ phase bilayers (not shown) at 343 K and 0% RH were analyzed successfully using the probability methods described by Dorset (1990), with the resulting electron-density maps presented in Figs. 2(*a*) and 2(*b*). Of the 11 orders that had to be assigned phases, only the third order could not be phased unambiguously. As such, in Fig. 2 we present absolute electron-density maps of the two possible phase combinations. Since the intensity of the third order is weak, its phase assignment is not critical, as is evident from Fig. 2 where the electron-density maps are virtually identical.

From the absolute one-dimensional electron-density distributions of 3D-L_δ phase DLPC bilayers at 343 K and 0% RH (Figs. 2*a* and 2*b*), we can observe the negative trough in the middle of the bilayer, due to the terminal methyl group, to be unusually shallow ($\simeq 0.23$ e Å^{-3}) when compared, for example, with 0% RH DPPC bilayers at 293 K (Katsaras & Stinson, 1990) and gel-phase multilamellar vesicles of DPPC in excess water at 293 K (Wiener, Suter & Nagle, 1989), both of which exhibit electron densities of ~ 0.21 e Å^{-3} (deeper negative trough). In the gel-phase DPPC bilayers, integrating the area of the negative trough (half of a Gaussian) gives rise to an average volume for each terminal methyl (V_{CH_3}) of approximately 50 Å^3 (Wiener *et al.*, 1989; Nagle & Wiener, 1988). Using the same relationship derived by Wiener *et al.* (1989), we calculate a V_{CH_3} of 46 (1) Å^3 for the 3D-L_δ phase bilayers using a ρ_{CH_2} of 0.33 e Å^{-3} and an area per lipid of 45.6 Å^2, obtained from the headgroups being distributed on a square lattice of edge 6.75 Å and determined directly from the diffraction pattern. This value of 46 Å^3 for V_{CH_3} is indicative of a more ordered phase compared with gel-phase DPPC bilayers. From the maps in Fig. 2, we can also observe that the electron-density peaks from the phosphorylcholine headgroups have amplitudes of 0.6 e Å^{-3}, the result of headgroups forming a two-dimensional lattice. In bilayers where the headgroups do not form any type of a lattice (*e.g.* L_α, L_β *etc.*), the electron densities found as a result of these moieties (0.47–0.49 e Å^{-3}) are considerably lower (Wiener & White, 1992; Katsaras & Stinson, 1990; Wiener *et al.*, 1989). However, it is important to note that the mean headgroup volumes [348 Å^3 for glycero phosphorylcholine, (Wiener *et al.*, 1989; Nagle & Wiener, 1988)] are approximately equal regardless of the structural phase that the bilayers are in (*e.g.* L_α, L_β or 3D-L_δ). Integrating the area under the bilayer, we obtain a value of 368 e per lipid using a lipid area of 45.6 Å^2. Since DLPC contains 342 e, we obtain 2.6 waters per lipid having a total volume of 79.6 Å^3 at 343 K. Assuming that the headgroup region (11.5–22.1 Å) in 3D-L_δ phase DLPC bilayers at 343 K and 0% RH (Fig. 2) also contains approximately 2.5 CH_2 groups (Pearson & Pascher, 1979) having a volume of 60.3 Å^3, we can calculate a mean

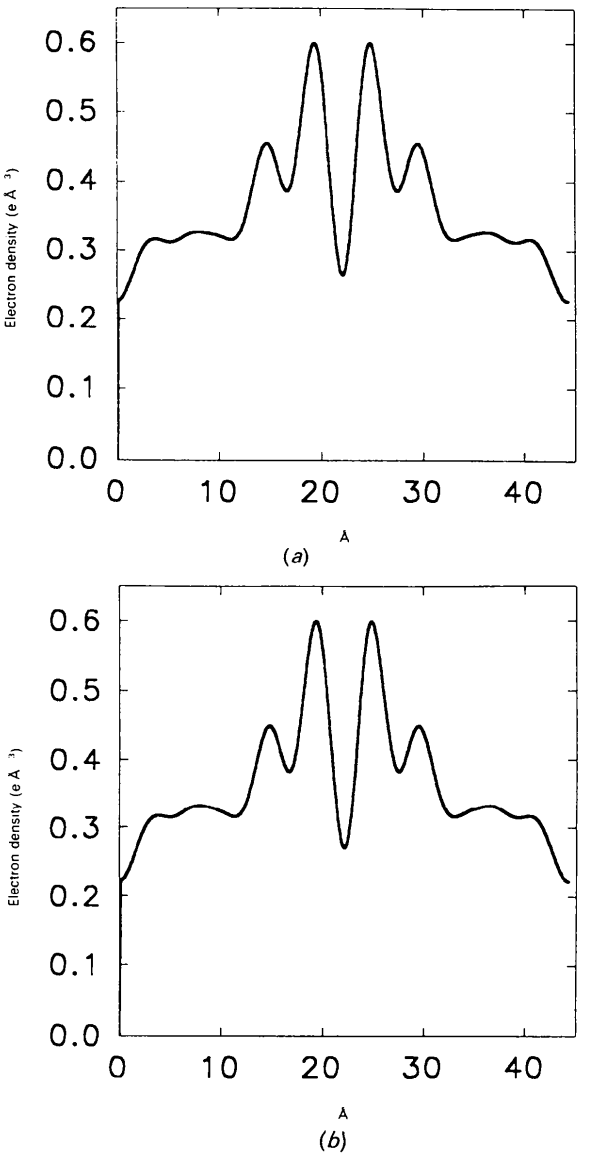

Fig. 2. Absolute electron-density profiles of oriented 3*D*-L_δ phase DLPC bilayers having a *d* spacing of 44.2 Å at 343 K and 0% RH. Since the third-order reflection could not unambiguously be phased, we present distributions for the two possible phase combinations. The phases for $h = 1$–11 (φ_h) are: (*a*) π, 0, 0, π, 0, π, 0, π, 0, π, 0; (*b*) $\varphi_3 = \pi$. The corrected structure-factor amplitudes for $h = 1$–11 are: 2629, 285, 67, 965, 252, 640, 694, 1370, 937, 630, 146. It is important to note that the maps were calculated using an average bilayer electron density of 0.365 instead of the predicted 0.367 e Å^{-3} in order to maintain 164 e per DLPC headgroup and a ρ_{CH_2} of approximately 0.33 e Å^{-3}.

headgroup volume of ~ 343 Å^3. These measurements support our methods for translating maps to an absolute scale. Finally, the distributions in Fig. 2 exhibit electron densities of ~ 0.33 e Å^{-3} on average in the region of the hydrocarbon tails. This value is slightly higher than gel-phase DPPC bilayers which have an approximate ρ_{CH_2} value of 0.32 e Å^{-3} (Katsaras & Stinson, 1990; Wiener *et al.*, 1989). The result is not unexpected since gel-phase bilayers give rise to wide-angle reflections of 1/4.2 instead of 1/4.4 Å^{-1}, indicative of hexagonal or near-hexagonal packing, and the methylene groups of which have a mean volume of ~ 25 compared with 24 Å^3 when the chains pack in an orthorhombic lattice [1/4.4 Å^{-1} (Nagle & Wiener, 1988; Small, 1984)].

At 343 K and RH's $\geq 30\%$, the oriented DLPC multilayers were in the L_α phase. In Fig. 3 we present the electron-density maps on an absolute scale for the DLPC bilayers at 30 and 100% RH's using the same methods as above to solve for the phase problem. This time, the only ambiguous phase assignments were for order numbers 2 and 5 for the sample at 30% RH and order numbers 5 and 9 for the 100% RH sample. However, we were able to obtain phase assignments for the second- and ninth-order reflections using the following methodology: with increasing levels of humidity there were slight changes in the lamellar spacing but considerable changes in intensity as a result of changes in the motif (data not shown). The intensity of order 2

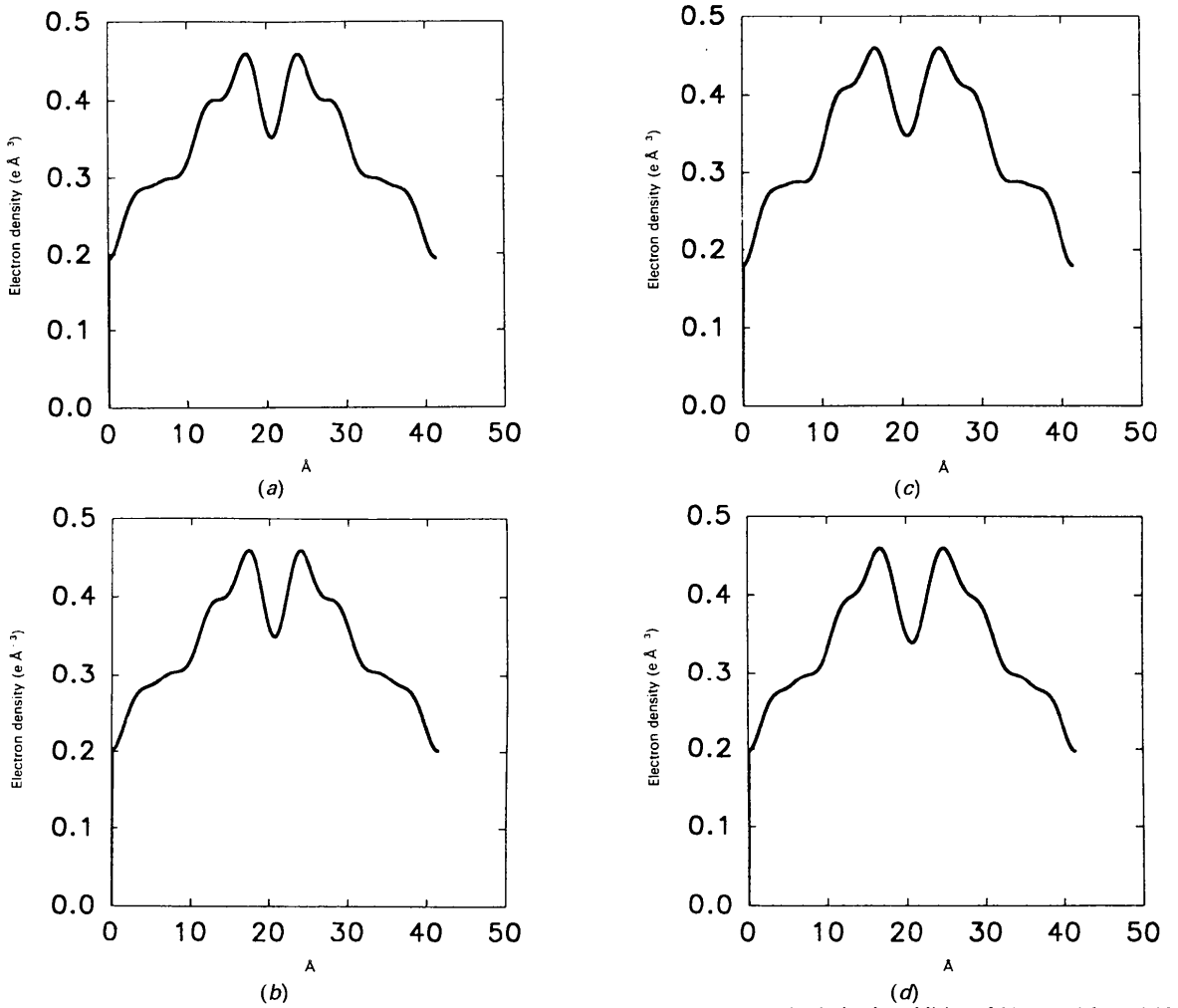

Fig. 3. Absolute electron-density profiles of oriented L_α phase DLPC bilayers at 343 K and relative humidities of 30 (*a* and *b*) and 100% (*c* and *d*) having *d* spacings of 41.3 and 41.4 Å, respectively. In these two cases (30 and 100% RH's), we were unable to successfully phase the fifth-order reflections and as such, we present the two possible electron-density distributions for each case as a result of the ambiguity. The phases for the 30% RH sample and $h = 1$–8 which are: (*a*) π, π, 0, π, π, π, 0, π; (*b*) $\varphi_5 = 0$. The bilayers at 30% RH have corrected structure-factor amplitudes for $h = 1$–8 which are: 2548, 310, 215, 698, 50, 424, 270, 328. The phases for the 100% RH sample and $h = 1$–9 are: (*c*) π, π, 0, π, π, π, 0, π, π; (*d*) $\varphi_5 = 0$. The corrected structure-factor amplitudes for the 100% RH sample are: 2308, 508, 429, 688, 93, 413, 167, 139, 123.

remained substantial at all humidities, suggesting that no phase change took place as the sample was hydrated. As such, the phase for the second-order reflection (φ_2) should be the same for all the samples at 343 K and RH's $\geq$ 30% (Torbet & Wilkins, 1976). Since φ_2 for the sample at 100% RH was calculated to be π, it then follows that φ_2 for the sample at 30% RH should also have a value of π. Since the fifth-order reflection could not be phased in either sample (30 or 100% RH), a similar argument could not be made for this reflection. In Figs. 3(*a*) and 3(*b*) we reconstructed the maps at 30% RH for $\varphi_5 = \pi$ or 0. The phase assignment of π for the ninth-order reflection of the 100% RH sample was made on the basis of consistency with the 30% RH maps. The phase for the ninth-order reflection of the 100% RH sample was deduced as follows: Since hydration did not alter the structure of the bilayer drastically (*e.g.* gel to liquid-crystalline phase transition), as judged from a particular reflection either consistently increasing, decreasing or not changing in intensity with increasing levels of humidity (data not shown), one would expect the various RH bilayer profiles to be similar. A phase assignment of π for the ninth-order reflection of the 100% RH sample at 343 K (Figs. 3*c* and 3*d*) provided such electron-density distributions. Again, the phase for the fifth-order Bragg reflection could not be assigned without any ambiguity.

Comparison of electron-density maps from 3D-L_δ phase bilayers (Figs. 2*a* or 2*b*) with those from bilayers in the L_α phase at 343 K (Figs. 3*a* or 3*b*) reveal the following differences: (*a*) a decrease in the electron densities of the hydrophobic tail region from $\sim$0.33 e Å^{-3} when the tails are in an orthorhombic packing in the 3D-L_δ phase to $\sim$0.29 e Å^{-3} in the disordered L_α phase. (*b*) The electron-density peak as a result of the terminal methyl groups (negative trough near the center of the bilayer deepened) decreases in the L_α phase to $\sim$0.19 from $\sim$0.23 e Å^{-3} in the 3D-L_δ phase. (*c*) The electron-density peak, which is primarily as a result of the phosphate moiety in the headgroup, decreases from 0.6 e Å^{-3} in the 3D-L_δ phase where the headgroups are distributed on a two-dimensional square lattice of edge $\sim$6.8 Å to 0.46 e Å^{-3} in the L_α phase where the headgroups do not possess any long-range order, the result of headgroup reorientation. (*d*) The L_α phase experiences a decrease in *d* spacing and bilayer thickness (phosphate-peak-to-phosphate-peak) of 2.9 and 5.0 Å, respectively, when compared with the 3D-L_δ phase.

A saturated hydrocarbon chain consists of a series of CH_2 groups and a terminal CH_3. The difference in electron density between the methylene groups of the fatty-acid chain and its terminal methyl group can easily be attributed to the volumes occupied by the two groups. In addition, the difference in electron densities after a phase transition is explained in a similar fashion. Our data of L_α-phase DLPC bilayers at 343 K (Figs. 3*a* or 3*b*) are in agreement with a recent paper by Wiener & White (1992), who translated the structure of L_α dioleoyl PC (DOPC, 18:1) bilayers to an absolute electron-density scale. From the absolute electron-density distributions in Fig. 3, we calculated in a similar fashion to the 0% RH bilayers at 343 K a V_{CH_3} of 50 (1) (Figs. 3*a* and 3*b*) and 52 (1) Å^3 (Figs. 3*c* and 3*d*) using values of 0.29 e Å^{-3} for ρ_{CH_2} and an area per lipid of 60.5 and 63.0 Å^2 for the 30 and 100% RH bilayers, respectively. The headgroup areas were calculated on the assumption of a constant lipid volume (Nagle & Wiener, 1988). Integrating the areas under the bilayers yielded 8.2 and 10.2 water (30.6 Å^3 per water at 343 K) molecules per lipid for bilayers at 30 (Figs. 3*a* and 3*b*) and 100% RH (Figs. 3*c* and 3*d*), respectively, with the negative water troughs having amplitudes of $\sim$0.35 e Å^{-3} for all the maps in Fig. 3. Again, this result compares favorably with L_α DOPC bilayers which contain approximately 5.4 waters per lipid and a negative water-trough amplitude of $\sim$0.37 e Å^{-3} (Wiener & White, 1992). With increasing waters per lipid, the overlap between the choline and phosphate groups of apposed bilayers will decrease creating a 'deeper' negative water trough of reduced electron density. In a similar fashion to the 3D-L_δ phase bilayers, headgroup volumes of approximately 348 and 338 Å^3 were calculated for the bilayers at 30 and 100% RH, respectively.

Unlike the samples at 343 K, the DLPC bilayers at 298 K did swell with increasing levels of hydration,

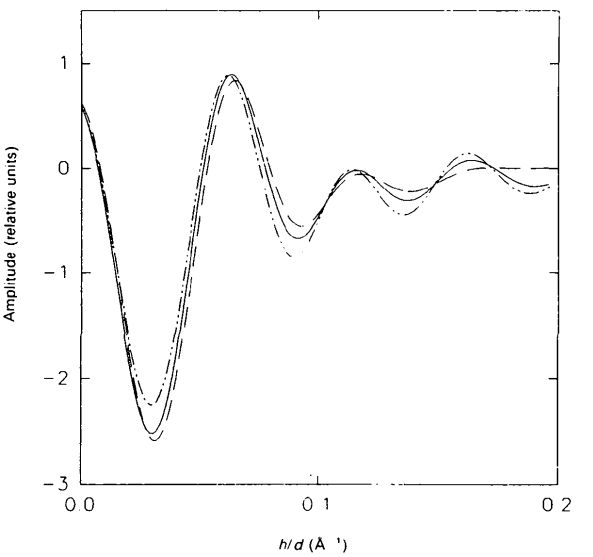

Fig. 4. Reconstructed continuous Fourier transforms of DLPC bilayers at 293 K and relative humidities of: (- - -) 70%; (—) 90%; (– –) 100%.

enabling us to phase the bilayers by plotting their structure factors in reciprocal space and calculating their continuous transforms using sampling theory (*e.g.* Katsaras & Stinson, 1990) for each swelling state (Fig. 4). This was necessary since the samples contained more than one phase at relative humidities of $<55\%$ and as such, not enough points could be obtained to map the continuous transform experimentally.

In Fig. 4 we present the calculated continuous transforms for three swelling states (70, 90 and 100% RH). If the motif (bilayer) remained unchanged, then one continuous transform would fit the data for all humidities. However, since the motif is not preserved during swelling, the bilayer thickness is decreased, then each swelling state is described correctly only by its own unique transform. The resulting family of transforms is simple and constant in nature. Any changes in the phase of a structure factor would result in destroying the simplicity and constancy (Torbet & Wilkins, 1976) of the three transforms. For example, the continuous transform indicated by the solid black line (90% RH) is in all reciprocal space 'sandwiched' between the two other transforms (70 and 100% RH). Changing the phase of any of the non-zero structure factors would result in eliminating that behaviour. With increasing levels of hydration the transforms expand uniformly in reciprocal space since the bilayers experience an almost uniform decrease in thickness.

The electron-density distributions derived from the transforms are presented in Fig. 5. Comparison of the electron-density distributions in Fig. 5 reveals recognizable increases in the water layer (5.7 Å) with increasing levels of humidity (70–100% RH). At the same time, one can observe a decrease of 3.3 Å in the thickness of the bilayers from 70 to 100% RH. DLPC bilayers at these humidities and this temperature are in the liquid-crystalline L_α phase (McIntosh, 1978) and their electron-density profiles compare favorably with the L_α-phase bilayers at 343 K and RH's of 30 and 100% in Fig. 3. The only noticeable difference between L_α bilayers at 293 (*e.g.* Fig. 4*a*) and 343 K (*e.g.* Fig. 3*a*) is in the region of the 'water layer' where the 343 K bilayers exhibit a higher electron density (~ 0.35 *versus* ~ 0.30 e Å^{-3}). This difference is the result of a larger number of waters per lipid present in the 293 K L_α bilayers (11.8–19.3 waters per lipid, 70–100% RH) compared with the L_α bilayers at 343 K (Fig. 3) and possible headgroup reorientation. The headgroup volumes for L_α DLPC bilayers at 293 K ranged from 348 Å^3 at 70% RH to

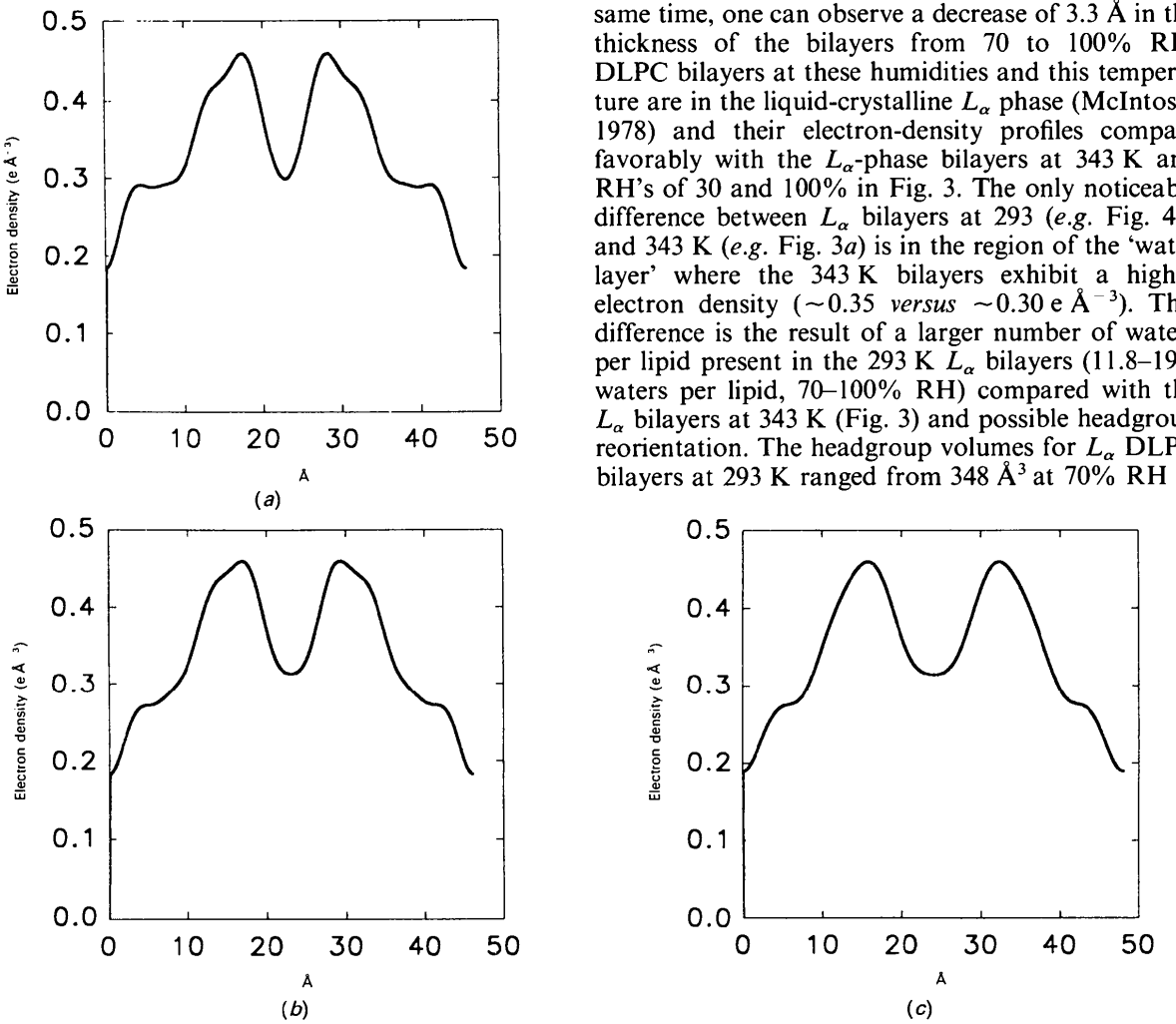

Fig. 5. Absolute electron-density profiles of oriented DLPC bilayers in the L_α phase at 293 K and relative humidities of: (*a*) 70%; (*b*) 90%; (*c*) 100%. The corrected structure factors are: (*a*) −1631, −809, 690, −736, −61, −359, 0, −58, −147 for 45.6 Å bilayers at 70% RH. (*b*) −1639, −1027, 723, −495, −111, −199, −69, 0, −133 for bilayers with a *d* spacing of 46.1 Å at 90% RH. (*c*) −1342, −1272, 596, −196, −220, −76, −134 for bilayers at 100% RH having a repeat spacing of 48.0 Å.

355 Å^3 at 100% RH using areas per lipid of 59.3 and 65.5 Å^2, respectively. Terminal methyl-group volumes increased with increased levels of humidity from 51 (1) at 70% RH to 56 (2) Å^3 at 100% RH.

In conclusion, we have clearly demonstrated, using one-dimensional absolute electron-density profiles calculated by means of direct-phasing methods, quantitative structural differences between two phases of DLPC. In addition to the changes observed by other researchers when comparing gel and liquid-crystalline bilayers, our profiles clearly show the phosphorylcholine headgroup reorienting when the DLPC bilayers undergo a transition from the 3D-L_δ phase to the L_α phase. Although a 2D-L_δ phase has been previously observed (Tardieu *et al.*, 1973), we have reported and quantified the physical characteristics for the first time of a DLPC 3D-L_δ phase which seems to differ substantially from the two-dimensional phase.

We are indebted to Dr Douglas L. Dorset for discussions and his critical reading of the manuscript. We would also like to thank D. S. C. Yang for use of his rotating-anode two-dimensional detector. JK is the recipient of a Natural Sciences and Engineering Research Council of Canada postdoctoral fellowship (NSERC). This research was supported by grants from NSERC.

References

ABRAHAMSSON, S., DAHLEN, B., LÖFGREN, H. & PASCHER, I. (1978). *Prog. Chem. Fats Other Lipids*, **16**, 125–143.
CHAPMAN, D., URBINA, J. & KEOUGH, K. M. (1974). *J. Biol. Chem.* **249**, 2512–2521.
DORSET, D. L. (1990). *Biophys. J.* **58**, 1077–1087.
DORSET, D. L. (1991*a*). *Biophys. J.* **60**, 1356–1365.
DORSET, D. L. (1991*b*). *Biophys. J.* **60**, 1366–1373.
DORSET, D. L., BECKMANN, E. & ZEMLIN, F. (1990). *Proc. Natl Acad. Sci. USA*, **87**, 7570–7573.
DOUCET, J., LEVELUT, A. M. & LAMBERT, M. (1983). *Acta Cryst.* B**39**, 724–731.
GENNIS, R. B. (1989). *Biomembranes: Molecular Structure and Function*. New York: Springer-Verlag.
HAUPTMAN, H. & KARLE, J. (1953). *Solution of the Phase Problem I. The Centrosymmetric Crystal*. ACA Monograph No. 3. Ann Arbor, MI: Edwards Brothers.
JENDRASIAK, G. L. & HASTY, J. H. (1974). *Biochim. Biophys. Acta*, **337**, 79–91.
KATSARAS, J. & STINSON, R. H. (1990). *Biophys. J.* **57**, 649–655.
KATSARAS, J., STINSON, R. H., DAVIS, J. H. & KENDALL, E. J. (1991). *Biophys. J.* **59**, 645–653.
KATSARAS, J., YANG, D. S.-C. & EPAND, R. M. (1992). *Biophys. J.* **63**, 1179–1175.
LUZZATI, V., GULIK-KRZYWICKI, T. & TARDIEU, A. (1968). *Nature (London)*, **218**, 1031–1034.
MCINTOSH, T. J. (1978). *Biochim. Biophys. Acta*, **513**, 43–58.
MORROW, M. R. & DAVIS, J. H. (1987). *Biochim. Biophys. Acta*, **904**, 61–70.
NAGLE, J. F. & WIENER, M. C. (1988). *Biochim. Biophys. Acta*, **942**, 1–10.
PEARSON, R. H. & PASCHER, I. (1979). *Nature (London)*, **281**, 499–501.
RUOCCO, M. J. & SHIPLEY, G. G. (1982). *Biochim. Biophys. Acta*, **691**, 309–320.
SAYRE, D. (1952). *Acta Cryst.* **5**, 843.
SHANNON, C. E. (1949). *Proc. Inst. Radio Eng. NY*, **37**, 10–21.
SHERWOOD, D. H. (1976). *Crystals, X-rays and Proteins*. London: Longman.
SMALL, D. M. (1984). *J. Lipid Res.* **25**, 1490–1500.
TANFORD, C. (1973). *The Hydrophobic Effect: Formation of Micelles and Biological Membranes*. New York: John Wiley.
TARDIEU, A., LUZZATI, V. & REMAN, F. C. (1973). *J. Mol. Biol.* **75**, 711–733.
TORBET, J. & WILKINS, M. H. F. (1976). *J. Theor. Biol.* **62**, 447–458.
WIENER, M. C. & WHITE, S. H. (1992). *Biophys. J.* **61**, 434–447.
WIENER, M. C., SUTER, R. M. & NAGLE, J. F. (1989). *Biophys. J.* **55**, 315–325.

Acta Cryst. (1994). B**50**, 216–220

Structure of 1,1,5,5-Tetranitro-[4]peristylane. Structure Solution from Molecular Packing Analysis

BY HERMAN L. AMMON, ZUYUE DU AND JAMES R. HOLDEN

Department of Chemistry and Biochemistry, University of Maryland, College Park, MD 20742, *USA*

AND LEO A. PAQUETTE

Department of Chemistry, The Ohio State University, Columbus, OH 43210, *USA*

(*Received* 4 *January* 1993; *accepted* 31 *August* 1993)

Abstract

The structure of the title compound, decahydro-2,2,5,5-tetranitro-1,6:3,4-dimethanocyclobuta[1,2:3,-4]dicyclopentene, $C_{12}H_{12}N_4O_8$, was solved with the molecular packing program *MOLPAK*, starting with an *AM*1-geometry-optimized model of an isolated molecule. The 20 best predicted crystal structures